Three-Coordinate Organoboron Compounds BAr_2R (Ar = Mesityl, R = 7-Azaindolyl- or 2,2′-Dipyridylamino-Functionalized Aryl or Thienyl) for Electroluminescent Devices and Supramolecular Assembly

Wen-Li Jia,[a] Dong-Ren Bai,[a] Theresa M^{c}Cormick,[a] Qin-De Liu,[a] Michael Motala,[a] Rui-Yao Wang,[a] Corey Seward,[a] Ye Tao,[b] and Suning Wang*[a]

Abstract: Eight novel three-coordinate boron compounds with the general formula BAr_2L, in which Ar is mesityl and L is a 7-azaindolyl- or a 2,2′-dipyridylamino-functionalized aryl or thienyl ligand, have been synthesized by Suzuki coupling, Ullmann condensation methods, or simple substitution reactions (L = *p*-(2,2′-dipyridylamino)-phenyl, **1**; *p*-(2,2′-dipyridylamino)biphenyl, **2**; *p*-(7-azaindolyl)phenyl, **3**; *p*-(7-azaindolyl)biphenyl, **4**; 3,5-bis(2,2′-dipyridylamino)phenyl, **5**; 3,5-bis(7-azaindolyl)phenyl, **6**; *p*-[3,5-bis(2,2′-dipyridylamino)phenyl]phenyl, **7**; 5-[*p*-(2,2′-dipyridylamino)phenyl]-2-thienyl, **8**). The structures of **1**, **3**, and **5**–**7** have been determined by X-ray diffraction analyses. These new boron compounds are bright blue emitters. Electroluminescent devices using compound **2** or **8** as the emitter and the electron-transport layer have been successfully fabricated. Molecular orbital calculations (Gaussian 98) have established that the blue emission of compounds **1**–**8** originates from charge transfer between the π orbital of the ligand L and the p_π orbital of the boron center. The ability of these boron compounds to bind to metal centers to form supramolecular assemblies was demonstrated by treatment of compound **2** with $Zn(O_2CCF_3)_2$, which generated a 1:1 chelate complex $\{\mathbf{2}\cdot Zn(O_2CCF_3)_2\}$ (**10**), and also by treatment of compound **4** with $AgNO_3$, yielding a 2:1 coordination compound $\{(\mathbf{4})_2\cdot Ag(NO_3)\}$ (**11**). In the solid state, compounds **10** and **11** form interesting head-to-head and tail-to-tail extended structures that host solvent molecules such as benzene.

Keywords: blue emitter · boron · coordination chemistry · luminescence · N ligands · OLEDs

Introduction

Three-coordinate organoboron compounds have recently emerged as an important and very promising class of materials for various photonic and optoelectronic applications.[1] Marder and others have carried out extensive studies on three-coordinate organoboron compounds and have demonstrated their potential uses as frequency-doubling materials in nonlinear optics.[2,3] Shirota and co-workers have recently reported several classes of very elegant three-coordinate organoboron compounds involving aryl and thienyl groups, and have demonstrated their uses as emitters and as electron-transport and hole-blocking materials in organic light-emitting diodes (OLEDs).[4] Yamaguchi, Tamao, and others have recently shown that three-coordinate organoboron compounds can be used as effective fluorescent sensors for Lewis donors such as fluoride.[5] These demonstrated applications of the previously reported three-coordinate organoboron compounds stem from three important and characteristic features of these molecules. First, the empty and relatively low-lying $2p_\pi$ orbital on the boron center makes the three-coordinate boron compounds good electron acceptors. The reversible binding of the boron compounds to an external electron donor (Lewis base) or electrons provides the capability of the three-coordinate boron compounds to act as fluorescent sensors for Lewis bases or as electron-transport materials in OLEDs. The presence of an internal electron donor group in the three-coordinate boron compounds produces polarized donor–acceptor electronic transition, a prerequisite for nonlinear optical applications. Second, the presence of luminescent chromophores makes it possible to use these three-coordinate boron compounds as emitters in OLEDs and fluorescent sensors as well. Third, the electron-

[a] Dr. W.-L. Jia, D.-R. Bai, T. M^{c}Cormick, Q.-D. Liu, M. Motala, Dr. R.-Y. Wang, C. Seward, Prof. Dr. S. Wang
Department of Chemistry, Queen's University
Kingston, Ontario, K7L 3N6 (Canada)
Fax: (+1) 613-533-6669
E-mail: wangs@chem.queensu.ca

[b] Dr. Y. Tao
Institute for Microstructural Science
National Research Council, Ottawa, K1A 0R6 (Canada)

Supporting information for this article is available on the WWW under http://www.chemeurj.org/ or from the author.

DOI: 10.1002/chem.200305579

deficient boron centers in the three-coordinate boron compounds are protected by bulky substituent groups, which provide the boron compounds with sufficient chemical stability for useful practical applications. Despite the attractive features and the demonstrated potential applications of three-coordinate organoboron compounds described above, examples of useful three-coordinate boron materials in photonic and optoelectronic applications remain scarce. Furthermore, although research in OLEDs has made tremendous progress in the past decade, with full-color display OLED devices emerging as commercial products, stable blue emitters and charge-transport materials (hole- or electron-transport) that are either transparent in the visible region or emit in the blue or near UV region are still in great demand in the OLEDs industry.[6] Alq_3 (q = 8-hydroxyquinolinato) is one of the best electron-transport materials.[6,7] However, its application in OLEDs is rather limited by its intense emission band in the green region. Shirota's work indicated that three-coordinate boron compounds (BAr_3) may be very valuable as electron-transport materials in OLEDs.[4] Based on these considerations, our group initiated research on new three-coordinate boron compounds for applications in OLEDs. We recently reported several blue luminescent BAr_3 molecules in which Ar is an extended π-conjugated ligand functionalized by a 2,2′-dipyridylamino chromophore.[8] Although these BAr_3 molecules are very bright blue emitters, attempts to use them in OLEDs were unsuccessful, due to the difficulty of vacuum-depositing these large molecular weight molecules onto the substrate. To overcome this problem, we have developed synthetic methods for new and relatively smaller molecules BAr_2R, where Ar = mesityl and R = 2,2′-dipyridylamino- or 7-azaindolyl-functionalized aryl or thienyl groups. The inclusion of 2,2′-dipyridylamino or 7-azaindolyl groups in the new boron compounds is based on two established facts[9]: 1) these two groups are efficient fluorescent chromophores in the UV/blue region (depending on the substituent groups), and 2) these two groups are capable of binding to Lewis acids such as a metal ion via the nitrogen donor site, thus providing the potential to act as building blocks for luminescent supramolecular materials. The new boron molecules can indeed be sublimed and show promising properties for OLEDs applications and coordination chemistry. Here we report the results of our comprehensive study of this class of new three-coordinate boron compounds.

Results and Discussion

Syntheses: The new organoboron compounds BAr_2L (Ar = mesityl, L = *p*-(2,2′-dipyridylamino)phenyl, **1**; *p*-(2,2′-dipyridylamino)biphenyl, **2**; *p*-(7-azaindolyl)phenyl, **3**; *p*-(7-azaindolyl)biphenyl, **4**; 3,5-bis(2,2′-dipyridylamino)phenyl, **5**; 3,5-bis(7-azaindolyl)phenyl, **6**; *p*-[3,5-bis(2,2′-dipyridylamino)-phenyl]phenyl, **7**; 5-[*p*-(2,2′-dipyridylamino)phenyl]-2-thienyl, **8**) can be divided into three groups. The first group contains a phenyl or a biphenyl group functionalized at the 4- or 4′-position either by a 2,2′-dipyridylamino or by a 7-azaindolyl group (compounds **1**–**4**; see Scheme 1). The second group contains a phenyl or a biphenyl functionalized by two 2,2′-dipyridylamino groups or two 7-azaindolyl groups at the 3- and the 5-positions or the 3′- and 5′-positions (compounds **5**–**7**). The third group contains a thienyl group functionalized by a *p*-(2,2′-dipyridylamino)phenyl group (compound **8**). As shown in Scheme 1, the first group of compounds was synthesized in good yields (78–90%) by treatment of the appropriate aryl bromide at −78°C with butyllithium (BuLi) and subsequently with BAr_2F (Ar = mesityl). The functionalized phenyl compounds **5** and **6** in the second group were obtained in good yield by a procedure similar to that used

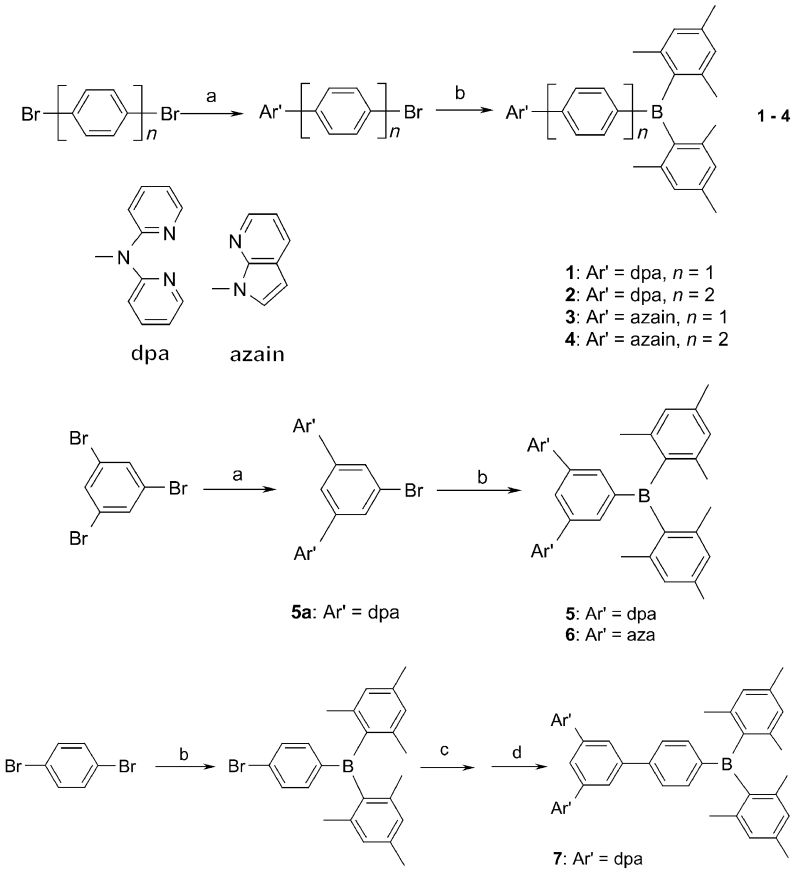

Scheme 1. a) 2,2′-Dipyridylamine or 7-azaindole, KOH (or K_2CO_3), $CuSO_4$, 210°C; b) *n*BuLi, $(Mes)_2BF$, −78°C; c) *n*BuLi, $B(OMe)_3$, −78°C; d) $[Pd(PPh_3)_4]$, **5a**, NaOH.

for **1**–**4**. The bis(2,2′-dipyridylamino)-substituted biphenyl compound **7** was obtained by a two-step reaction. First, 1,4-dibromobenzene was treated with one equivalent of BuLi and one equivalent of BAr_2F to produce BAr_2(4-Br-phenyl), which was converted into the boronic acid BAr_2(4-$B(OH)_2$-phenyl) by treatment with BuLi and $B(OCH_3)_3$ at −78 °C. Through the use of Pd-catalyzed Suzuki–Miyaura cross-coupling reactions[10] and $[Pd(PPh_3)_4]$ as the catalyst in the presence of NaOH, the reaction of BAr_2(4-$B(OH)_2$-phenyl) with 1-bromo-3,5-bis(2,2′-dipyridylamino)benzene produced compound **7** in 21% yield. Compound **8** was obtained by two different methods, as shown in Scheme 2. The first method involves treatment of *p*-(2,2′-dipyridylamino)-2-thienylbenzene (**8a**) with BuLi and BAr_2F at −78 °C, producing **8** in a relatively low yield (25%). The second method involves treatment of *p*-(2,2′-dipyridylamino)phenyl-2-bromo-5-thiophene (**8b**) with BuLi and BAr_2F at −78 °C, producing compound **8** in 62% yield.

The starting materials, aromatic bromide compounds, were prepared in moderate yields (43–68%) by treatment of *p*-dibromobenzene, *p*-dibromobiphenyl, or 1,3,5-tribromobenzene with 7-azaindole or 2,2′-dipyridylamine by Ullmann condensation methods with K_2CO_3/KOH and $CuSO_4$ as a base and a catalyst, respectively[11] (Scheme 1). The significant factors in the synthesis of these aromatic bromides are the reaction temperatures and reaction times. For example, for the synthesis of 3,5-di-(2,2′-dipyridylamino)-1-bromobenzene, if the reaction temperature is not sufficiently high (<190 °C), no reaction occurs. If the reaction temperature is too high (>210 °C) or the reaction time too long (>12 h), the main product is 1,3,5-tris-(2,2′-dipyridylamino)benzene. If the reaction time is shorter than 5 h, monosubstituted compound is the main product. The optimum reaction conditions are 200–205 °C, 10 h with a 1:2 ratio of 1,3,5-tribromobenzene and 2,2′-dipyridylamine. The ligand **8a** was prepared by treatment of 2-thienylzinc bromide with *p*-(2,2′-dipyridylamino)-bromophenyl in the presence of $[Pd(PPh_3)_2Cl_2]$ and diisobutylaluminium hydride in ≈60% yield. The ligand **8b** was prepared by Suzuki–Miyaura cross-coupling[10] of 2,5-dibromothiophene and *p*-(2,2-dipyridylamino)phenylboronic acid in 80% yield. The syntheses of the ligands and the three groups of boron compounds are summarized in Scheme 1.

Crystal structures: The new boron compounds **1**–**8** were fully characterized by NMR and elemental analyses. To establish the full structural parameters to aid our investigation into the relationship of structures and electronic properties, we also carried out structural determination by single-crystal X-ray diffraction methods for compounds **1**, **3**, and **5**–**7**, which produced suitable single crystals. Crystal data are provided in Table 1. Selected bond lengths and angles for these compounds are provided in Table 2. The structures of **1**, **3**, and **5**–**7** are shown in Figures 1, 2, 3, 4, and 5, respectively.

The boron centers in all five structures adopt nearly ideal trigonal planar geometries. The largest deviation from the ideal trigonal planar geometry was observed in compound **7**, in which the C-B-C angles range from 113.7(7)° to 128.7(7)°. The B(mesityl)$_2$ units in all five structures are not coplanar with their adjacent phenyl rings. The dihedral angles between the BC_3 planes and the adjacent phenyl rings are 26.9, 26.3, 24.2, 28.6, and 30.0° in **1**, **3**, **5**, **6**, and **7**, respectively. Similar dihedral angles have been observed in (mesityl)$_2$B-aryl-B(mesityl)$_2$ compounds reported by Marder and co-workers.[2a] The lack of coplanarity between BC_3 unit and phenyl ring can be attributed to steric interactions imposed by the methyl groups. Figures 1–5 show clearly that the boron centers in these compounds are well protected by the methyl groups of the mesityl ligands. The amino nitrogen atoms of the 2,2′-dipyridylamino units in compounds **1**, **5**, and **7** adopt typical trigonal planar geometries. However, the NC_3 planes of the amino nitrogens in all three compounds are not coplanar with the adjacent phenyl rings, as is evident from the dihedral angles, ranging from 43.9 to 89.3°. The lack of coplanarity between the 2,2′-dipyridylamino groups and the phenyl rings is apparent in the side view of molecule **5** as shown in Figure 3b, in which the pyridyl groups are oriented above and below the central phenyl ring, respectively. In contrast, the dihedral angles between the 7-azaindolyl units and the adjacent phenyl rings in **3** and **6** are much smaller (38.9° in **3**, 39.7° and 40.1° in **6**), due to much reduced steric interactions. The biphenyl unit in **7** is not coplanar, but with a dihedral angle between the two phenyl rings of 20.2°. Previously we have reported a number of symmetrically 1,3,5-substituted starburst molecules based on benzene or triazine frameworks and involving 2,2′-dipyridylamino or 7-azaindolyl substituent groups.[9a] Compounds **5** and **6** can be viewed as new starburst molecules with two different types of substituents—an electron-donor substituent (dipyridylamino or 7-azaindolyl) and an electron-acceptor substituent (BAr_2)—coexisting in the same molecule. The B−C and N−C bond lengths in compounds **1**, **3**, and **5**–**7** are typical and similar to previously reported three-coordinate boron compounds and 2,2′-dipyridylamino or 7-azaindolyl

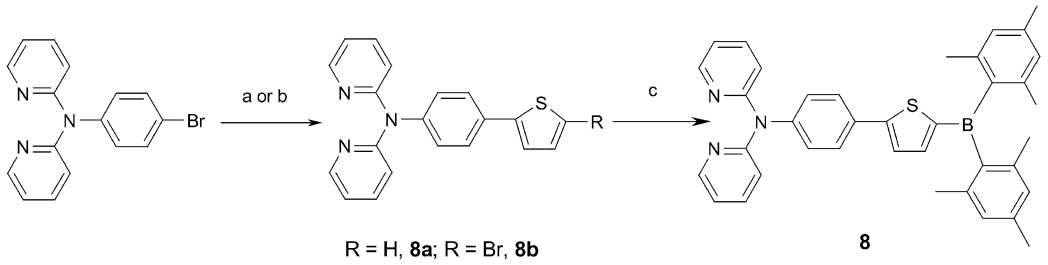

Scheme 2. a) 2-Thienylzinc bromide, DIBAH, $[Pd(PPh_3)_2Cl_2]$; b) 1) *n*BuLi, $B(OMe)_3$, −78 °C, 2) 2,5-dibromothiophene, $[Pd(PPh_3)_4]$, Na_2CO_3; c) *n*BuLi, $(Mes)_2BF$, −78 °C.

Table 1. Crystallographic data.

	1	**3**	**5**	**6**	**7**	**10**	**11**
formula	$C_{34}H_{34}BN_3$	$C_{31}H_{31}BN_2$	$C_{44}H_{41}BN_6$	$C_{38}H_{35}BN_4{\cdot}0.5\,CH_2Cl_2$	$C_{50}H_{45}BN_6{\cdot}2\,CH_2Cl_2$	$C_{44}H_{38}BF_6N_3O_4Zn{\cdot}C_6H_6$	$C_{74}H_{70}B_2N_5O_3Ag{\cdot}3\,C_6H_6{\cdot}0.5\,C_6H_{14}$
fw	495.45	442.39	664.64	600.97	910.58	941.10	1477.19
T (K)	297	298	298	298	293	295	180
space group	$Pna2_1$	$P2_1$	$P\bar{1}$	$P\bar{1}$	$P\bar{1}$	$P\bar{1}$	$P\bar{1}$
a [Å]	11.179(3)	12.224(4)	11.144(2)	12.011(2)	8.234(2)	8.8127(17)	10.146(4)
b [Å]	22.942(7)	13.231(4)	12.088(3)	12.182(2)	15.670(4)	10.2718(19)	16.490(6)
c [Å]	11.332(3)	16.429(5)	15.629(3)	23.384(5)	20.651(5)	26.996(5)	23.695(8)
α [°]	90	90	104.225(3)	98.554	67.439(15)	79.591(3)	94.309(6)
β [°]	90	102.940	103.158(4)	100.405(4)	81.303(19)	87.205(3)	97.831(7)
γ [°]	90	90	104.981(4)	95.243(5)	88.36(2)	87.065(4)	98.899(6)
V [Å^3]	2906.1(14)	2589.6(13)	1873.7(7)	3303.3(11)	2431.2(11)	2398.4(8)	3861(2)
Z	4	4	2	4	2	2	2
ρ_{calcd} [g cm^{-3}]	1.132	1.135	1.178	1.208	1.244	1.303	1.270
μ [mm^{-1}]	0.066	0.065	0.070	0.149	0.285	0.581	0.317
$2\theta_{max}$ [°]	56.56	56.74	56.60	56.74	57.42	56.60	56.72
no. of rflns measured	19908	18705	13585	24156	15296	17025	27214
no. of rflns used (R_{int})	6632 (0.0476)	10086 (0.0322)	8590 (0.0330)	15241 (0.0369)	10705 (0.369)	10771 (0.0182)	17451 (0.0422)
no. of parameters	343	613	460	788	567	635	871
final R ($I>2\sigma(I)$), $R1$[a]	0.0415	0.0589	0.0530	0.0926	0.1066	0.0475	0.0996
$wR2$[b]	0.0872	0.1396	0.1068	0.2540	0.1209	0.1136	0.2630
R (all data) $R1$[a]	0.1432	0.1161	0.1901	0.2427	0.5128	0.0928	0.1932
$wR2$[b]	0.1053	0.1597	0.1376	0.3019	0.1994	0.1270	0.2888
Good. of fit on F^2	0.757	0.872	0.778	0.835	0.708	0.893	1.058

[a] $R1 = \Sigma[|F_o|-|F_c|]/\Sigma|F_o|$. [b] $wR2 = \{\Sigma[w(F_o^2-F_c^2)]/\Sigma(wF_o^2)\}^{1/2}$, $w = 1/[\sigma^2(F_o^2) + (0.075P)^2]$, where $P = [\mathrm{Max}(F_o^2,0) + 2F_c^2]/3$

derivatives.[8,9] No significant intermolecular π stacking interactions are observed in any of the five structures.

Physical properties: All eight new boron compounds are stable in solution and in the solid state upon extended exposure to air. This remarkable chemical stability in this class of molecules is attributable to the presence of the bulky mesityl groups and is consistent with the behavior of previously reported BAr_3 molecules with bulky protecting groups.[1–5,12] These new boron compounds also exhibit remarkable thermal stability, with melting points ranging from 141 °C (**7**) to 260 °C (**2**). Glass transition temperatures were observed for compounds **1** (T_g = 81 °C), **2** (T_g = 132 °C), and **3** (T_g = 68 °C) by DSC analyses, indicating that these new boron compounds are capable of forming amorphous phases. Despite repeated attempts, no glass transition temperatures were observed for compounds **4**–**8**. The glass-forming capability of similar three-coordinate boron compounds has previously been extensively examined by Shirota et al.[4g] Compounds **1**–**8** have moderate solubility in CH_2Cl_2 and are only slightly soluble in THF.

Electronic properties: Compounds **1**–**8** are colorless and each has a characteristic broad absorption band in the 300–400 nm region, which can be attributed to ligand→boron charge-transfer transitions. Sharp and intense absorption bands in the 200–300 nm region are also observed for **1**–**8**, and can be assigned to ligand-centered π–π* transitions. The UV/Vis absorption bands are given in Table 3. Compounds **1**–**8** display both reversible reduction peaks and pseudo-reversible oxidation peaks in cyclic voltammetry measurements. The reduction potentials were measured in THF solutions. No reduction potentials could be obtained for some of the compounds, due to poor solubility in THF. The oxidation potentials were measured in CH_2Cl_2 solutions. The reduction potentials (versus Ag/AgCl) of **1**–**8** were determined to be at −1.60 V to −1.84 V, while the first oxidation potentials of **1**–**8** were found to span a considerable range (1.20 V to 1.80 V). For compounds **5** and **7**, two pseudo-reversible (the heights of i_c and i_a are not symmetrical) oxidation peaks (1.23 V and 1.54 V for **5**; 1.54 V and 1.88 V for **7**) were observed, presumably due to two consecutive oxidations of the two 2,2′-dipyridylamino groups on the phenyl and the biphenyl moieties. For compound **8**, two pseudo-reversible oxidation peaks at 1.20 V and 1.68 V were observed, and could be attributed to the oxidation of the thiophene ring and the 2,2′-dipyridylamino group, respectively. The bipolar behavior of compounds **1**–**8** resembles that of three-coordinate boron compounds reported by Shirota et al.[4] From the redox potentials obtained by cyclovoltammetry measurements and the absorption edges of the UV/Vis spectra, we obtained the HOMO and LUMO energy levels for compounds **1**–**8** (with the ferrocene oxidation potential as the standard for the vacuum energy level[13]). The results are listed in Table 4, which shows for the first group of boron compounds (**1**–**4**) that the 2,2′-dipyridylamino-substituted compounds have somewhat higher HOMO levels and smaller band gaps than the 7-azaindolyl analogues. Similarly, the 2,2′-dipyridylamino-substituted compound **5** has a higher HOMO level than the 7-azaindolyl analogue, compound **6**.

Table 2. Selected bond lengths [Å] and angles [°] for compounds **1**, **3**, **5**–**7**, and **10**–**11**.

Compound **1**			
B(1)−C(14)	1.552(4)	C(14)-B(1)-C(26)	118.4(2)
B(1)−C(26)	1.575(4)	C(14)-B(1)-C(17)	120.8(2)
B(1)−C(17)	1.582(4)	C(26)-B(1)-C(17)	120.7(2)
Compound **3**			
B(1)−C(11)	1.566(5)	C(11)-B(1)-C(14)	117.9(3)
B(1)−C(14)	1.586(5)	C(11)-B(1)-C(23)	119.7(3)
B(1)−C(23)	1.567(5)	C(23)-B(1)-C(14)	122.4(3)
Compound **5**			
B(1)−C(1)	1.573(4)	C(1)-B(1)-C(10)	121.5(2)
B(1)−C(10)	1.577(3)	C(1)-B(1)-C(19)	119.1(2)
B(1)−C(19)	1.574(4)	C(19)-B(1)-C(10)	119.4(2)
Compound **6**			
C(1)−B(1)	1.586(7)	C(10)-B(1)-C(1)	122.4(5)
C(10)−B(1)	1.567(7)	C(19)-B(1)-C(1)	120.5(5)
C(19)−B(1)	1.547(8)	C(19)-B(1)-C(10)	117.1(4)
Compound **7**			
B(1)−C(10)	1.508(11)	C(10)-B(1)-C(19)	113.7(7)
B(1)−C(19)	1.605(10)	C(10)-B(1)-C(1)	128.6(7)
B(1)−C(1)	1.616(11)	C(19)-B(1)-C(1)	117.3(8)
Compound **10**			
B(1)−C(33)	1.563(4)	C(33)-B(1)-C(5)	117.6(2)
B(1)−C(5)	1.576(4)	C(33)-B(1)-C(14)	119.7(2)
B(1)−C(14)	1.580(4)	C(5)-B(1)-C(14)	122.7(2)
Zn(1)−O(1)	1.922(2)	O(1)-Zn(1)-O(3)	96.30(10)
Zn(1)−O(3)	1.931(2)	N(3)-Zn(1)-N(1)	91.20(8)
Zn(1)−N(3)	1.995(2)	C(5)-B(1)-C(14)	122.7(2)
Zn(1)−N(1)	1.9993(18)	C(5)-B(1)-C(14)	122.7(2)
Compound **11**			
B(1)−C(29)	1.565(9)	C(29)-B(1)-C(17)	118.8(5)
B(1)−C(17)	1.582(9)	C(29)-B(1)-C(20)	123.9(5)
B(1)−C(20)	1.582(9)	C(17)-B(1)-C(20)	117.3(5)
B(2)−C(54)	1.555(8)	C(54)-B(2)-C(57)	120.0(5)
B(2)−C(57)	1.569(9)	C(54)-B(2)-C(66)	115.9(5)
B(2)−C(66)	1.575(9)	C(57)-B(2)-C(66)	124.1(5)
Ag(1)−N(4)	2.236(6)	N(4)-Ag(1)-N(2)	150.9(3)
Ag(1)−N(2)	2.237(6)	O(2)-Ag(1)-O(1)	49.6(4)
Ag(1)−O(2)	2.473(11)		
Ag(1)−O(1)	2.533(11)		

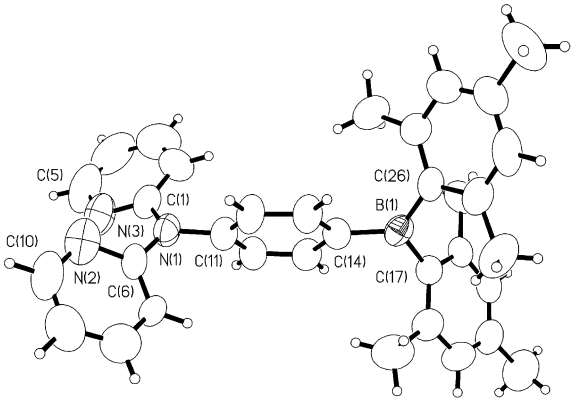

Figure 1. Molecular structure of compound **1** with labeling schemes.

The thienyl-containing compound **8** has the smallest band gap.

Luminescence: Compounds **1**–**8** each emit an intense blue color in solution and in the solid state when irradiated by

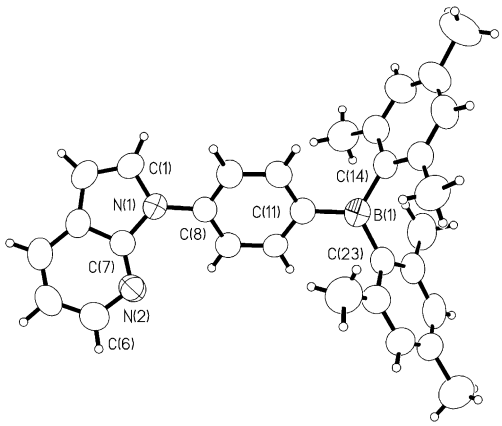

Figure 2. Molecule structure of compound **3** with labeling schemes.

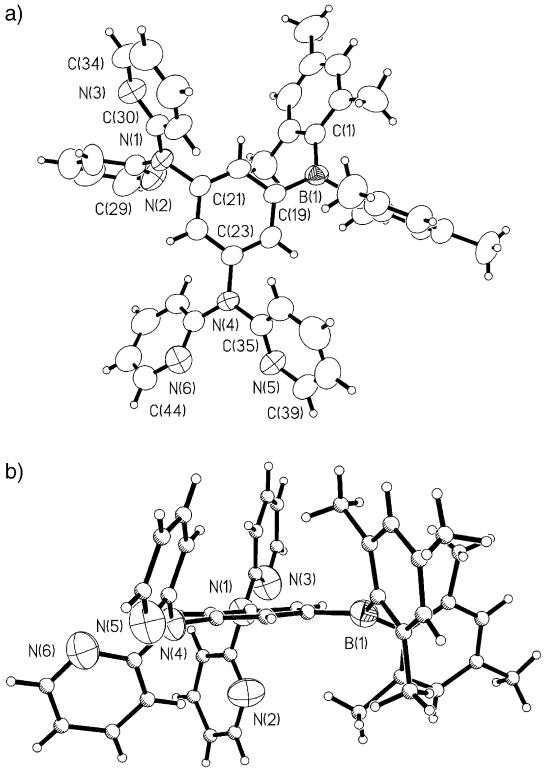

Figure 3. a) Molecular structure of compound **5** with labeling schemes. b) Side view of compound **5**.

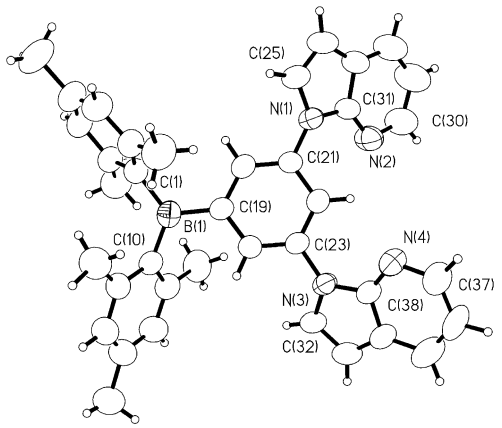

Figure 4. Molecular structure of compound **6** with labeling schemes.

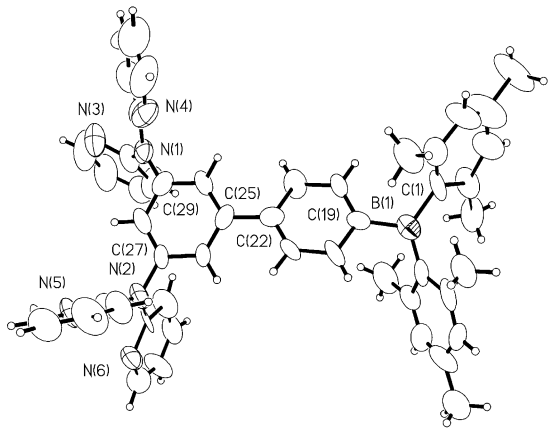

Figure 5. Molecular structure of compound **7** with labeling schemes.

Table 3. Absorption and luminescence data for compounds **1–8**.

Compd	UV/Vis absorption [nm] (ε, $M^{-1}cm^{-1}$)[a]	Excitation wavelength [nm]	Emission λ_{max} [nm]	Quantum yields (ϕ)[b]	Conditions 298 K
1	230 (19720), 250 (11760), 320 (12540), 362 (23850)	360	411	99	CH_2Cl_2
		384	417		solid
2	232 (48250), 270 (35660), 336 (40330)	351	449	63	CH_2Cl_2
		354	440		solid
3	230 (22630), 286 (7750), 336 (17670)	338	381	21	CH_2Cl_2
		348	398		solid
4	230 (38621), 256 (17230), 338 (49230)	357	413	66	CH_2Cl_2
		349	463		solid
5	230 (65650), 266 (53630), 302 (64990)	345	448	17	CH_2Cl_2
		320	449		solid
6	230 (75990), 258 (90420), 298 (23630), 336 (23480)	345	410	11	CH_2Cl_2
		348	418(sh),[c] 456		solid
7	304 (very broad, 64102)	355	456	6	CH_2Cl_2
		359	433		solid
8	230 (40720), 310 (20090), 382 (44490)	381	465	100	CH_2Cl_2
		418	469		solid

[a] All data were collected for CH_2Cl_2 solution ([M] = 1.0×10^{-5}–1.0×10^{-6}) at ambient temperature. [b] Relative to 9,10-diphenylanthracene in CH_2Cl_2 at ambient temperature. [c] sh = shoulder.

Table 4. HOMO and LUMO energy levels for compounds **1–9**.

Compound	HOMO [eV]	LUMO [eV]	Experimental band gap (eV)	HOMO from MO calculation (Hartree)	LUMO from MO calculation (Hartree)	Band gap from MO calculation (Hartree)
1	−5.7	−2.5	3.2	−0.19528	−0.06048	0.13480
2	−5.7	−2.5	3.2			
3	−6.1	−2.7	3.4	−0.20940	−0.05429	0.15511
4	−5.8	−2.5	3.3			
5	−5.5	−2.1	3.4	−0.19022	−0.05891	0.13131
6	−6.0	−2.6	3.4			
7	−5.8	−2.6	3.2			
8	−5.5	−2.6	2.9			
9				−0.20155	−0.07473	0.12682

UV light. In CH_2Cl_2, the emission maxima of **1–8** range from 381 nm (**3**) to 465 nm (**8**). In solution, the emission maxima change with changes in solvent polarity, a commonly observed phenomenon for three-coordinate organoboron compounds and attributable to the presence of a highly polarized excited state.[1–5] The absorption and emission spectra of compound **2** in THF and DMF are provided in Figure 6 as a representative example to demonstrate the solvent effect, the emission maximum of **2** shifting from 449 nm in THF to 475 nm in DMF. The 7-azaindolyl-substituted compounds emit at a higher energy than the corresponding 2,2′-dipyridylamino-substituted compounds, consistently with the trend in the band gaps determined by UV/Vis spectra. Compounds **1**, **2**, **4**, and **8** are the brightest emitters among this group of molecules, based on their quantum yields measured in CH_2Cl_2 with 9,10-diphenylanthracence as the standard. From their emission lifetimes, the emission of the boron compounds **1–8** at ambient temperature is fluorescence. As an example, the decay lifetime of compound **2** was determined at Photon Technology International (Canada) Inc. to be 1.113(4) ns, an indication of fluorescent emission. Because of the lack of easy access to facilities for fluorescent decay lifetime measurement, the fluorescent emission lifetimes of the remaining compounds were not measured. However, from their structural similarity, we believe that they all should probably have decay lifetimes in the ns time domain.

Molecular orbital calculations: To have a better understanding of the electronic and luminescent properties of compounds **1–8**, we carried out ab initio molecular orbital calculations on four representative compounds: BAr_2(*p*-(2,2′-dipyridylamino)phenyl) (**1**), BAr_2(*p*-(7-azaindolyl)-phenyl) (**3**), BAr_2(1,3-bis(2,2′-dipyridylamino)-phenyl) (**5**), and a model compound BAr_2(5-(2,2′-dipyridylamino)-2-thienyl) (**9**). The geometric parameters from X-ray diffraction analysis were used for the calculations for compounds **1**, **3**, and **5**. Because of the lack of X-ray data for compound **8**, geometric parameters for **8** could only be obtained by molecular modeling and geometric optimization. To minimize the computational time required for these calculations, we performed the calculation for the related but smaller molecule **9** (synthetic efforts to obtain this molecule were not successful). The geometric parameters for **9** were obtained by molecular modeling and geometric optimization. The Gaussian suite of programs[14] (Gaussian 98) was employed for the cal-

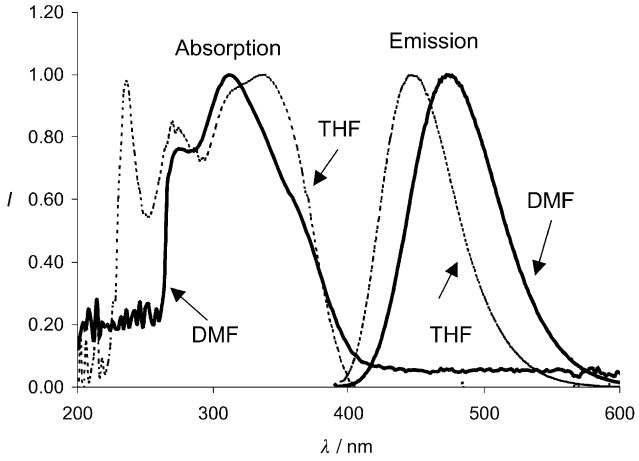

Figure 6. Absorption and emission spectra of compound **2** in THF and DMF.

culations. The calculations were performed with the 6–31G* basis set[15] at an RHF (restricted Hartree–Fock) level of computation. The orbital diagrams were generated by use of the Molekel program.[16] All contour values are ± 0.03 a.u. The calculated HOMO and LUMO energy levels and band gaps for **1**, **3**, **5**, and **9** are provided in Table 4. Compound **9** has the smallest calculated band gap, consistently with the experimentally observed trend for compounds **1**–**8**. The smaller band gap of the thienyl compounds **8** and **9** could be attributable to the effective conjugation between the boron center and the thienyl group, effectively lowering the LUMO level, hence the band gap. The LUMO levels for all compounds predominately consist of the empty p_π orbital on the boron center with substantial contribution of π^* orbitals from the phenyl or the thienyl portion of the luminescent ligand. The HOMO levels for all compounds are π orbitals involving the entire luminescent ligand. The HOMO and LUMO orbitals for **1**, **5**, and **9** (HOMO and LUMO orbitals of **3** are omitted) are shown in Figure 7. LUMO orbitals confirm the presence of conjugation between the π orbitals of the phenyl (or thienyl) portion of the 2,2′-dipyridylamino-functionalized ligand and the empty p_π orbital of the central boron atom. This is consistent with the fact that the B–C (phenyl) bond lengths for most of the structures determined by X-ray diffraction are slightly shorter than those of B–mesityl bonds (with the exception of compound **7**, in which the B–C (thienyl) bond appears to be longer than one of the B–C (mesityl) bonds. Because of the poor quality of data for **7**, however, there is much uncertainty on the bond lengths listed for **7** in Table 2.). The MO calculation results established unambiguously that the electronic transitions responsible for the emission of compounds **1**–**8** originate from the π orbitals of the 2,2′-dipyridylamino- or 7-azaindolyl-functionalized ligands to the π^* orbitals involving both boron and the luminescent ligand.

Electroluminescence: Compound **2** was chosen as a representative example of compounds **1**–**7** for the study of electroluminescent (EL) properties because of the following considerations: 1) compound **2** has the highest melting point and the highest T_g (132 °C), 2) compound **2** is one of the brightest emitters of compounds **1**–**7**, and 3) the emission maximum ($\approx$450 nm) of **2** in solution (CH_2Cl_2) and in the

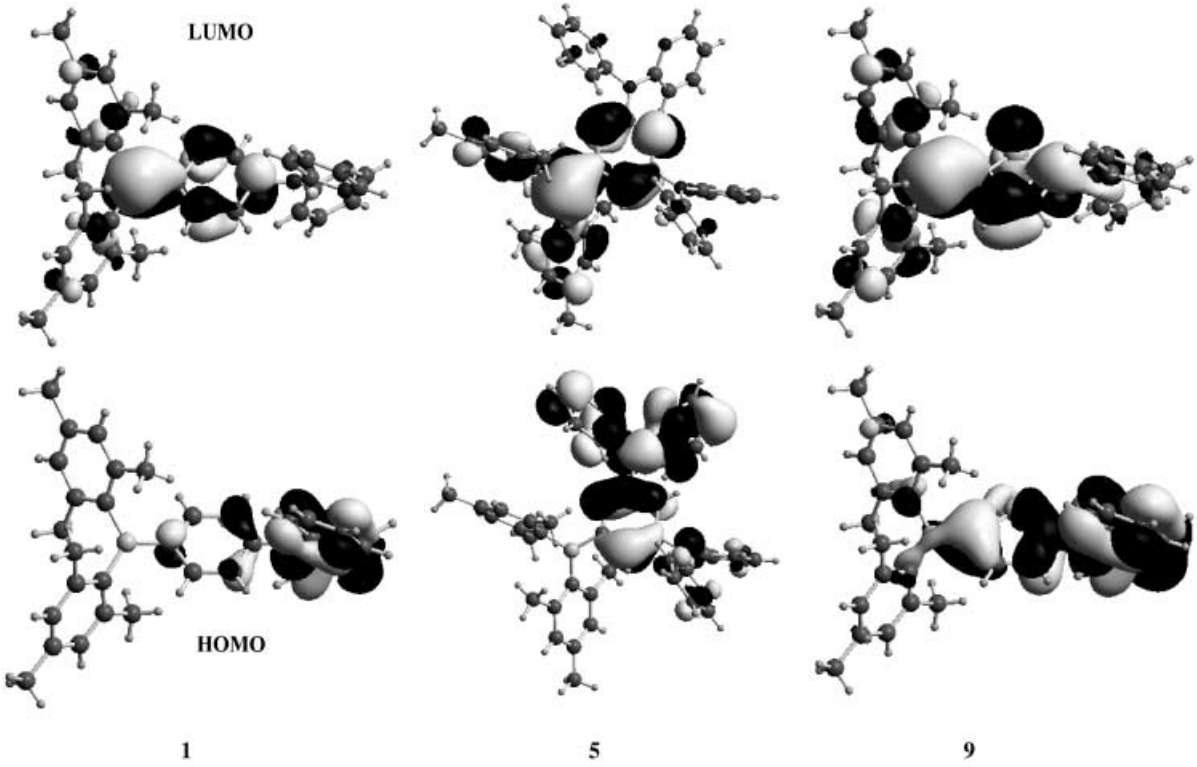

Figure 7. A diagram showing the HOMO and LUMO levels of compounds **1**, **5**, and **9**.

solid state (≈440 nm) is in the ideal blue emission region (430–450 nm). These three features make compound **2** the best candidate out of compounds **1**–**7** as a blue emitter for OLEDs. The presence of the thienyl group in compound **8** makes it a unique member among the eight new boron compounds reported here, so compound **8** was also chosen for the study of electroluminescent properties. Three types of EL devices were fabricated for compound **2**. Device 1 is a double-layer device consisting of ITO (indium-tin-oxide)/NPB (40 nm)/**2** (40 nm)/LiF (2 nm)/Al, where NPB (*N,N′*-di-1-naphthyl-*N,N′*-diphenylbenzidine) functions as a hole-transport layer. This device produces a bright whitish-blue emission with the EL maximum at 436 nm, which matches well with that of PL (Figure 8). The turn-on voltage of device 1 is 5 V and the maximum luminance is 2566 Cd m^{-2}

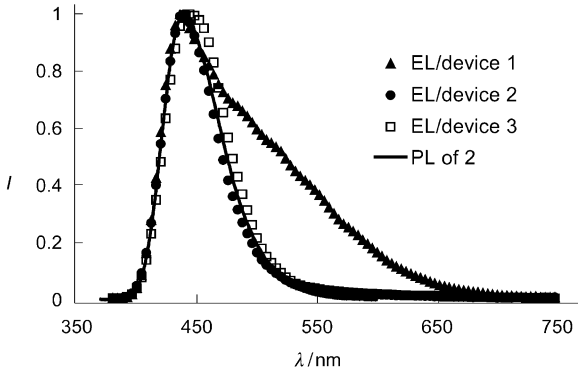

Figure 8. EL of devices 1–3 and PL of compound **2**.

at 17 V, indicating that device 1 is efficient and bright (Figures 9 and 10). The fact that no electron-transport material was used for device 1 indicates that the boron compound **2** can function both as an emitter and as an electron-transport material. The broad shoulder in the 500–700 nm region of the EL spectrum of device 1 is believed to originate from exciplex emission between the NPB and compound **2** layers. To remove the exciplex emission, device 2 was constructed, in which a bicarbazole hole-blocking layer[17] was inserted between the NPB layer and compound **2** (ITO/NPB (40 nm)/Bicarb (20 nm)/**2** (40 nm)/LiF (1 nm)/Al). As shown in Figure 8, the EL spectrum of device 2 matches the PL

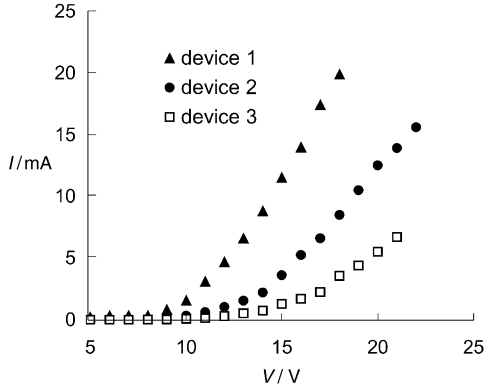

Figure 9. I–V diagrams for devices 1–3.

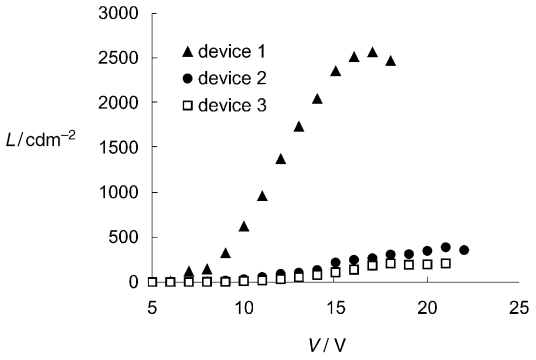

Figure 10. L–V diagrams of devices 1–3.

spectrum of **2** very well, confirming that the broad shoulder emission in device 1 is indeed from exciplex formation between NPB and compound **2**. The turn-on voltage for device 2 is 6 V and the maximum brightness is 388 Cd m^{-2} at 21 V. To improve the efficiency of the device further, an electron-transport layer—PBD (2-(4-biphenyl)-5-(4-*tert*-butylphenyl)-1,3,4-oxadiazole)—was added in device 3 (ITO/NPB (40 nm)/Bicarb (20 nm)/**2** (40 nm)/PBD (20 nm)/LiF (1 nm)/Al). The EL spectrum of device 3 is the same as that of device 2 and the PL of compound **2**. Device 3 is much less efficient than device 2, however (turn-on voltage, 7 V, maximum brightness, 208 ca m^{-2} at 21 V). This could be due to the fact that the LUMO level (−2.4 eV) of PBD is slightly above that (−2.5 eV) of **2**, which makes PBD an ineffective electron-transport material for the boron compound.

One type of EL device (device 4) for compound **8** was fabricated, based on the EL information obtained for compound **2**. Device 4 consists of ITO/NPB (40 nm)/bicarb (20 nm)/**8** (40 nm)/LiF (1 nm)/Al. Device 4 produces a bright blue emission with the EL maximum at 460 nm. The EL and the PL spectra of **8** match very well (Figure 11). The turn-on voltage of device 4 is 7 V (Figures 12 and 13). The maximum brightness is 1510 Cd m^{-2} at 24 V (Figure 13). Although the maximum luminance of the EL devices of compounds **2** and **8** may not be as high as in some of the blue EL devices reported previously, the new boron compounds are very promising for applications in OLEDs due to their capability to play dual roles—both as blue emitters and as electron-transport materials—in the EL devices, as demonstrated by EL devices 1–4. Further device modification and

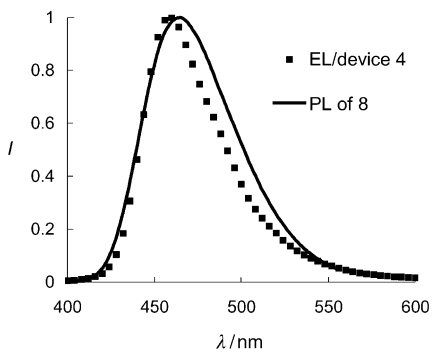

Figure 11. EL of device 4 and PL of compound **8**.

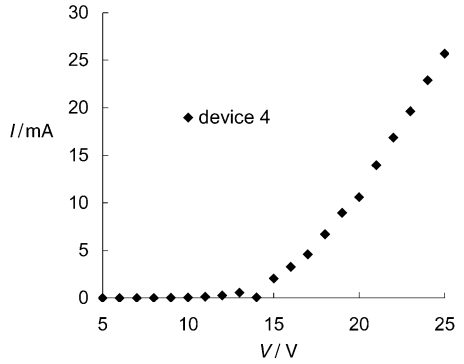

Figure 12. I–V diagram of device 4.

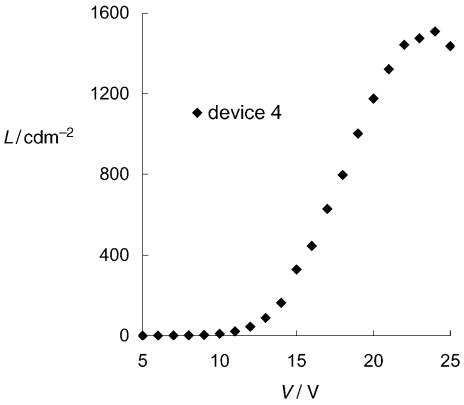

Figure 13. L–V diagram of device 4.

optimization could lead to better performance of these important materials in OLEDs.

Coordination and supramolecular architectures: Lewis acidity represents the typical reactivity of most previously known three-coordinate boron compounds.[5] One unique feature that distinguishes compounds **1**–**8** from the previously reported three-coordinate boron compounds is the presence of Lewis base sites. In the 7-azaindolyl-containing compounds **3**, **4**, and **6**, the nitrogen atoms in the six-membered rings of the 7-azaindolyl groups have lone pairs of electrons and are capable of binding to Lewis acids such as metal ions as a terminal ligand. In contrast, in the 2,2′-dipyridylamino-containing compounds **1**, **2**, **5**, **7**, and **8**, the two pyridyl groups of the 2,2′-dipyridylamino units can function as bidentate chelate ligands to bind to metal ions. Our previous investigation into luminescent organic molecules containing 7-azaindolyl or 2,2′-dipyridylamino groups showed that interactions of metal ions with these groups often lead to substantial changes in luminescence (emission energy shift or quenching, depending on the metal ion involved).[9] Since the emission of compounds **1**–**8** originates from a polarized transition (ligand π orbital to π* dominated by boron p_π orbital), as established by the experimental data and molecular orbital calculations, binding of the 7-azaindolyl or 2,2′-dipyridylamino groups in compounds **1**–**8** to metal ions may have effects on the emission of the boron compounds. To investigate this, we synthesized two representative complexes: a zinc(II) complex of molecule **2**—{BAr_2(*p*-(2,2′-dipyriylamino)-biphenyl)}[$Zn(O_2CCF_3)_2$] (**10**)—and a silver(I) complex of molecule **4**—{BAr_2(*p*-(7-azaindolyl)-biphenyl)}$_2$($AgNO_3$) (**11**). Complex **10** was obtained by treatment of compound **2** with $Zn(O_2CCF_3)_2$ in a 1:1 ratio while compound **11** was obtained by treatment of compound **4** with $AgNO_3$ in a 1:1 ratio. Both compounds were fully characterized by NMR and X-ray diffraction analyses.

As shown in Figure 14, the $Zn(O_2CCF_3)_2$ unit in **10** is chelated to the two pyridyl groups of the 2,2′-dipyridylamino unit (a diagram with labeling scheme for **10** is available in the Supporting Information). The Zn^{II} ion has a distorted tetrahedral geometry with bond angles ranging from

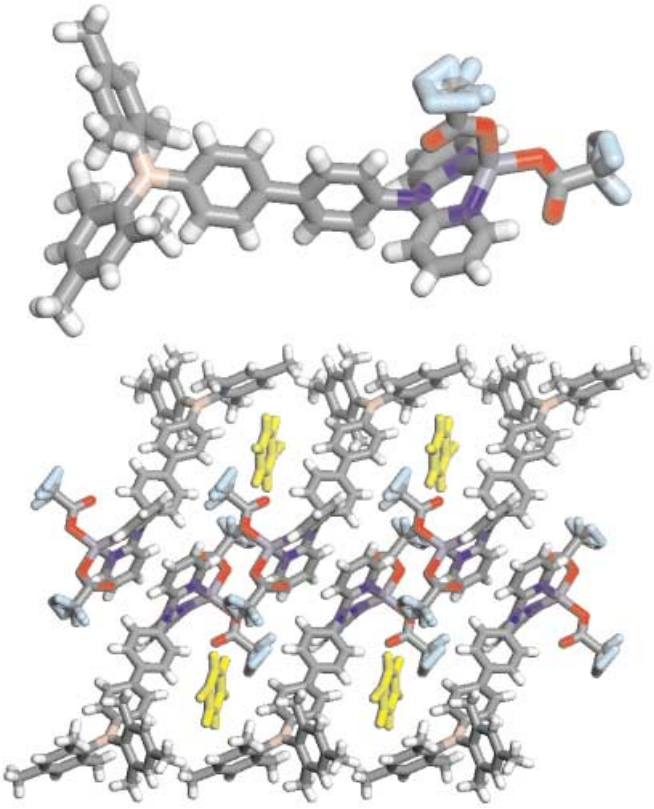

Figure 14. Top: The molecular structure of compound **10**. Bottom: Unit cell packing diagram showing the solvent channels in the crystal of **10** (N: blue; B: orange; Zn: gray-blue; O: red; F: light green; solvent molecules: yellow).

91.20(8)° (N(1)-Zn(1)-N(3)) to 125.89(9)° (O(1)-Zn(1)-N(1)) and typical bond lengths.[9b,c] In the crystal lattice, molecules of **10** are arranged in a head-to-head and tail-to-tail manner such that void channels are formed. Benzene solvent molecules are trapped in the channels (one benzene per molecule of **10**; Figure 14). The trapped benzene solvent molecules are remarkably stable and had not escaped from the crystal lattice even after the crystals had been isolated from the solution and kept at ambient temperature for weeks. In fact, after being kept under vacuum for two days, the crystals of **10** still contained one benzene molecule per molecule of **10**, as revealed by CHN analysis. Space-filling drawing shows that the benzene solvent channels are partial-

ly blocked by molecules of **10**, which apparently hinder the escape of the solvent molecules. It is very likely that the $Zn(O_2CCF_3)_2$ unit interacts in the same manner with other 2,2′-dipyriylamino-containing molecules (**1**, **5**, **7**, **8**).

The structure of **11** is shown in Figure 15 (a diagram with labeling scheme for **11** is available in the Supporting Information). The $AgNO_3$ unit is bound to two 7-azaindolyl groups from two molecules of **4**. Although a 1:1 ratio of **4** and $AgNO_3$ was used in the synthesis, only the 2:1 product was isolated, which is attributable to the tendency of the Ag^I ion to achieve coordination saturation, thus binding to two 7-azaindolyl groups. The coordination geometry around the Ag^I center is irregular, with a large N(1)-Ag^I-N(2) angle (150.9(3)°) and normal Ag–N bond lengths.[18] The nitrate group is chelated to the Ag^I ion through two relatively long Ag–O bonds (Ag(1)–O(1) = 2.533(11), Ag(1)–O(2) = 2.473(11) Å). Similar Ag–O bond distances have been observed previously.[18–19] The two 7-azaindolyl-biphenyl groups linked by the $AgNO_3$ unit are almost parallel with the 7-azaindolyl group, being situated almost directly above the neighboring biphenyl unit. The shortest atomic separation distance between these two groups is 3.39 Å, indicating the presence of significant π–π stacking interactions. As can be seen in the crystal lattice of **11** (Figure 15), the inorganic portion involving the $AgNO_3$ unit in compound **11** stacks together, while the organic portion of **11** stacks together in the crystal lattice. As a result of such stacking, solvent channels that host benzene and hexane (the hexane disordered and not fully resolved by X-ray diffraction analysis) are formed within the crystal lattice (Figure 15). The solvent molecules in the crystals of **11** partially escape from the lattice at ambient temperature. However, after prolonged drying under vacuum, some of the solvent molecules were still found in the crystalline sample, as verified by CHN analysis results (see Experimental Section). Again, this relative stability of the trapped solvent molecules in crystals of **11** can be attributed to partial blockage of the solvent channels by molecules of **11**.

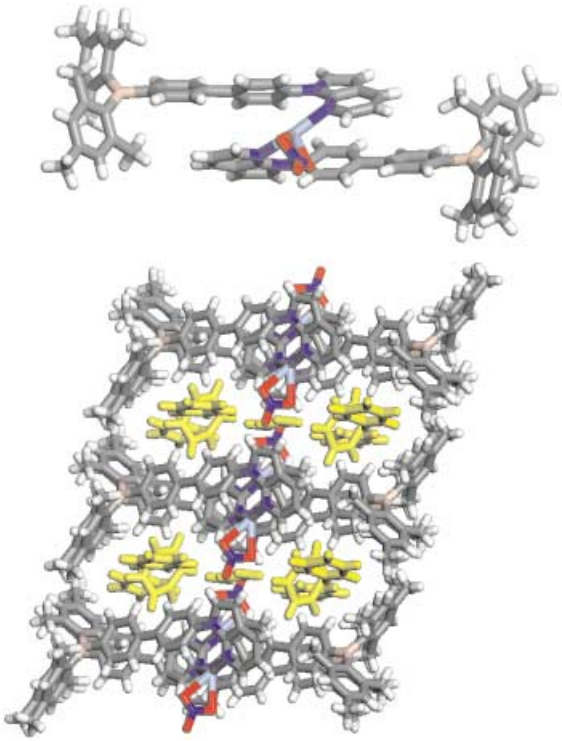

Figure 15. Top: The molecular structure of **11**. Bottom: Unit cell packing diagram showing the solvent channels in the crystal of **11** (N: blue; B: orange; Zn: gray-blue; O: red; F: light green; solvent molecules: yellow).

The luminescent properties of complexes **10** and **11** are similar to those of compounds **2** and **4**, respectively, in solution and in the solid state. For a given solvent, the emission peaks of compounds **10** and **11** are essentially identical to those of **2** and **4**, respectively. The emission spectra of compounds **10** and **11** display solvent-dependent shifts similar to those of compounds **2** and **4**. The emission intensities of **10** and **11** are only slightly lower than those of **2** and **4** at the same concentrations. Emission spectral measurements for solutions containing compounds **2** and $Zn(O_2CCF_3)_2$ of various ratios were conducted, and showed (Figure 16) that significant emission intensity decrease only occurs when the ratio of **2** and $Zn(O_2CCF_3)_2$ is less than 1:2, attributable to the presence of dissociation/association equilibria between the $Zn(O_2CCF_3)_2$, molecules of **2**, and complex **10** in solution. $AgNO_3$ was found to have a similar effect on the emission of compound **4**. These data led us to conclude that metal ions such as Zn^{II} and Ag^I do not significantly alter the emission energy of the three-coordinate boron compounds **1**–**8**, but do partially quench their emission intensities, by coordinating to the nitrogen donor site. Compounds such as **10** and **11** may be useful as fluorescent sensors for small organic molecules because of their luminescence and their porous structures in the solid state. This is currently being explored in our laboratory.

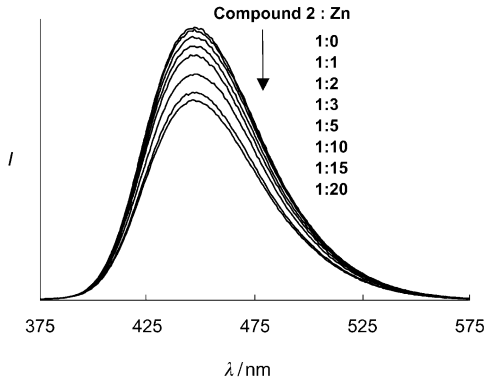

Figure 16. The emission spectral change of compound **2** in THF in the presence of various amounts of $Zn(O_2CCF_3)_2$.

Conclusion

A new class of chemically and thermally stable, three-coordinate boron compounds has been developed. We have demonstrated that the members of this new class of boron

compounds are bright blue emitters and are capable of functioning in OLEDs both as blue emitters and as electron-transport materials. Charge-transfer transitions from the luminescent ligand to the p_π orbital of the boron center are primarily responsible for the observed luminescence. By utilizing the Lewis base sites of 7-azaindolyl and 2,2′-dipyridylamino, these new boron molecules can function as ligands to bind to metal centers such as Ag^I and Zn^{II}. As a consequence of such metal–ligand interactions, the emission intensities of the boron compounds are partially quenched and interesting extended structures that can host molecules such as benzene in the solid state have been obtained. Further improvements on EL devices based on the new boron compounds and further investigation into the usage of the new boron compounds as building blocks for the formation of new luminescent supramolecular structures and their potential applications in fluorescent sensors will be conducted.

Experimental Section

All starting materials were purchased from Aldrich Chemical Company and were used without further purification. Solvents were freshly distilled over appropriate drying reagents. All experiments were carried out under a dry nitrogen atmosphere by use of standard Schlenk techniques unless otherwise stated. TLC was carried out on silica gel. Flash chromatography was carried out on silica (silica gel 60, 70–230 mesh). ^{1}H and ^{13}C NMR spectra were recorded on Bruker Avance 300 or 500 MHz spectrometers. ^{19}F NMR spectra were recorded on a Bruker Avance 400 MHz spectrometer. Excitation and emission spectra were recorded on a Photon Technologies International QuantaMaster Model 2 spectrometer. Elemental analyses were performed by Canadian Microanalytical Service Ltd., Delta, British Columbia, Canada. Melting points were determined on a Fisher–Johns melting point apparatus. All DSC measurements were performed on a Perkin Elmer Pyris DSC 6. Cyclic voltammetry was performed on a BAS CV-50W analyzer with scan rates of 100 mV s^{-1}. The electrolytic cell used was a conventional three-compartment cell, with a Pt working electrode, Pt auxiliary electrode, and Ag/AgCl reference electrode. All experiments were performed at room temperature with 0.10 M tetrabutylammonium hexafluorophosphate (TBAP)/acetonitrile as the supporting electrolyte. The ferrocenium/ferrocene couple was used as the internal standard. Aromatic bromides, *p*-(2,2′-dipyridylamino)bromobenzene,[11a] *p*-(2,2′-dipyridylamino)bromobiphenyl,[11a] *p*-(7-azaindolyl)bromobenzene,[11a] *p*-(7-azaindolyl)bromobiphenyl,[11a] 3,5-bis(7-azaindolyl)-bromobenzene,[20] and *p*-(2,2′-dipyridylamino)phenylboronic acid[8] were synthesized by previously reported procedures.

Synthesis of 3,5-bis(2,2′-dipyridylamino)bromobenzene (5a): A mixture of 2,2′-dipyridylamine (2.4 g, 14.1 mmol), 1,3,5-tribromobenzene (2.2 g, 7.0 mmol), $CuSO_4 \cdot 5H_2O$ (0.17 g), and K_2CO_3 (2.9 g, 21.0 mmol) was heated under N_2 at 206 °C for 8 h. The mixture was extracted with CH_2Cl_2 (3 × 25 mL) and the solvent was removed in vacuo. The residue was passed through a column on silica gel with ethyl acetate/hexane (6:1) as the eluent. The first fraction was 1,3-dibromo-5-(2,2′-dipyridylamino)-benzene (11% yield). The second fraction was the target compound 3,5-bis(2,2′-dipyridylamino)bromobenzene (43% yield). The third was 1,3,5-tris(2,2′-dipyridylamino)benzene (14% yield).

^{1}H NMR of 3,5-bis(2,2′-dipyridylamino)bromobenzene ($CDCl_3$, 25 °C): δ = 8.37 (dd, J = 5.1, 1.2 Hz, 4H), 7.62 (ddd, J = 8.4, 7.5, 1.8 Hz, 4H), 7.12 (d, J = 1.8 Hz, 2H), 7.06 (dt, J = 8.4, 0.9 Hz, 4H), 6.99 (ddd, J = 7.2, 5.1, 0.9 Hz, 4H), 6.92 (t, J = 1.8 Hz, 1H) ppm.

^{1}H NMR of 1,3-dibromo-5-(2,2′-dipyridylamino)benzene ($CDCl_3$, 25 °C): δ = 8.39 (d, J = 3.7 Hz, 2H), 7.65 (ddd, J = 8.1, 7.5, 1.9 Hz, 2H), 7.48 (t, J = 1.8 Hz, 1H), 7.25 (d, J = 1.8 Hz, 2H), 7.00–7.06 (m, 4H) ppm.

Synthesis of *p*-(2,2′-dipyridylamino)phenyldimesitylborane (1): A hexane solution of *n*BuLi (1.6 M, 1.3 mL, 2.08 mmol) was added at −78 °C to a solution of *p*-(2,2′-dipyridylamino)bromobenzene (0.652 g, 2 mmol) in THF (20 mL), and the mixture was stirred for 1 h at that temperature. A solution of dimesitylboron fluoride (0.595 g, 90%, 2.0 mmol) in Et_2O (20 mL) was added to the mixture. The reaction mixture was stirred for 1 h at −78 °C, allowed slowly to reach room temperature, and stirred overnight. The solvents were removed under reduced pressure. The residue was subjected to column chromatography on silica gel (THF/hexane, 1:2) to afford colorless compound **1** in 87% yield; m.p. 196–198 °C; ^{1}H NMR ($CDCl_3$, 25 °C): δ = 8.45 (d, J = 3.6 Hz, 2H), 7.63 (ddd, J = 8.1, 7.5, 1.8 Hz, 2H), 7.53 (d, J = 8.4 Hz, 2H), 7.11 (d, J = 8.4 Hz, 2H), 7.00–7.05 (m, 4H), 6.84 (s, 4H), 2.32 (s, 6H), 2.08 (s, 12H) ppm; ^{13}C NMR ($CDCl_3$, 25 °C): δ = 158.2, 149.1, 142.3, 141.4, 139.2, 139.0, 138.9, 138.7, 128.8, 125.1, 119.7, 118.6, 105.8, 24.2, 21.8 ppm; elemental analysis calcd (%) for $C_{34}H_{34}BN_3$: C 82.46, H 6.87, N 8.49; found: C 82.26, H 7.00, N 8.32.

Syntheses of Compounds 2–6 and 7a: These compounds were obtained by a procedure similar to that described for compound **1**. All boron compounds were recrystallized from CH_2Cl_2 and hexane.

***p*-(2,2′-Dipyridylamino)biphenyldimesitylborane (2)**: Yield 90%; m.p. 260–261 °C; ^{1}H NMR ($CDCl_3$, 25 °C): δ = 8.43 (d, J = 3.3 Hz, 2H), 7.69 (d, J = 8.4 Hz, 2H), 7.60–7.65 (m, 6H), 7.29 (d, J = 8.4 Hz, 2H), 6.98–7.05 (m, 4H), 6.86 (s, 4H), 2.34 (s, 6H), 2.06 (s, 12H) ppm; ^{13}C NMR ($CDCl_3$, 25 °C): δ = 158.7, 149.0, 145.7, 145.0, 144.2, 142.2, 141.3, 139.3, 138.0, 137.9, 137.6, 128.7, 127.8, 126.9, 126.1, 118.9, 117.7, 23.2, 21.5 ppm; elemental analysis calcd (%) for $C_{40}H_{38}BN_3 \cdot 0.5\,CH_2Cl_2$: C 79.22, H 6.36, N 6.85; found: C 79.46, H 6.68, N 6.59.

***p*-(7-Azaindolyl)phenyldimesitylborane (3)**: Yield 85%; m.p. 161–162 °C; ^{1}H NMR ($CDCl_3$, 25 °C): δ = 8.42 (d, J = 4.8 Hz, 1H), 8.01 (dd, J = 7.8, 1.5 Hz, 1H), 7.89 (d, J = 8.1 Hz, 2H), 7.71 (d, J = 8.1 Hz, 2H), 7.63 (d, J = 3.6 Hz, 1H), 7.18 (dd, J = 7.8, 4.8 Hz, 1H), 6.86 (s, 4H), 6.68 (d, J = 3.6 Hz, 1H), 2.35 (s, 6H), 2.08 (s, 12H) ppm; ^{13}C NMR ($CDCl_3$, 25 °C): δ = 147.6, 143.7, 143.1, 141.8, 141.0, 138.8, 138.1, 129.4, 128.6, 128.4, 128.1, 127.6, 122.4, 117.1, 102.7, 23.7, 21.4 ppm; elemental analysis calcd (%) for $C_{31}H_{31}BN_2$: C 84.20, H 7.02, N 6.34; found: C 84.12, H 7.04, N 6.30.

***p*-(7-Azaindolyl)biphenyldimesitylborane (4)**: Yield 78%; m.p. 184–186 °C; ^{1}H NMR ($CDCl_3$, 25 °C): δ = 8.44 (dd, J = 4.8, 1.5 Hz, 1H), 8.03 (dd, J = 7.8, 1.5 Hz, 1H), 7.90 (dd, J = 6.6, 2.1 Hz, 2H), 7.83 (dd, J = 6.6, 2.1 Hz, 2H), 7.63–7.67 (m, 4H), 7.59 (d, J = 3.6 Hz, 1H), 7.19 (dd, J = 7.8, 4.8 Hz, 1H), 6.87 (s, 4H), 6.70 (d, J = 3.6 Hz, 1H), 2.35 (s, 6H), 2.08 (s, 12H) ppm; ^{13}C NMR ($CDCl_3$, 25 °C): δ = 147.8, 144.2, 144.0, 142.5, 141.2, 139.5, 139.3, 138.6, 137.8, 130.2, 129.0, 128.9, 128.8, 128.5, 127.2, 124.8, 122.6, 117.5, 102.7, 24.2, 21.9 ppm; elemental analysis calcd (%) for $C_{37}H_{35}BN_2$: C 85.71, H 6.76, N 5.40; found: C 85.37, H 6.96, N 4.88.

3,5-Bis(2,2′-dipyridylamino)phenyldimesitylborane (5): Yield 58%; m.p. 224–226 °C; ^{1}H NMR ($CDCl_3$, 25 °C): δ = 8.30 (dd, J = 4.8, 1.2 Hz, 4H), 7.53 (ddd, J = 8.4, 6.6, 1.8 Hz, 4H), 7.14 (t, J = 2.1 Hz, 1H), 7.11 (d, J = 2.1 Hz, 2H), 6.98 (d, J = 8.4 Hz, 4H), 6.90 (dd, J = 6.6, 5.1 Hz, 4H), 6.72 (s, 4H), 2.25 (s, 6H), 2.04 (s, 12H) ppm; ^{13}C NMR ($CDCl_3$, 25 °C): δ = 158.3, 149.6, 148.8, 146.2, 142.0, 141.4, 139.5, 138.2, 131.9, 129.6, 128.8, 118.9, 117.6, 24.1, 21.8 ppm; elemental analysis calcd (%) for $C_{44}H_{41}BN_6$: C 79.54, H 6.18, N 12.65; found: C 78.85, H 6.11, N 12.51.

3,5-Bis(7-azaindolyl)phenyldimesitylborane (6): Yield 67%; m.p. 196–198 °C; ^{1}H NMR ($CDCl_3$, 25 °C): δ = 8.83 (t, J = 2.1 Hz, 1H), 8.34 (dd, J = 4.8, 1.5 Hz, 2H), 7.98 (dd, J = 7.8, 1.5 Hz, 2H), 7.73 (d, J = 2.1 Hz, 2H), 7.54 (d, J = 3.6 Hz, 2H), 7.13 (dd, J = 7.8, 4.8 Hz, 2H), 6.87 (s, 4H), 6.63 (d, 3.6 Hz, 2H), 2.34 (s, 6H) 2.15 (s, 12H) ppm; ^{13}C NMR ($CDCl_3$, 25 °C): δ = 148.2, 144.2, 141.8, 141.7, 139.9, 139.8, 129.7, 129.2, 129.1, 128.9, 128.7, 124.0, 122.3, 117.4, 102.4, 24.4, 22.0 ppm; elemental analysis calcd (%) for $C_{38}H_{35}BN_4 \cdot 0.5\,CH_2Cl_2$: C 76.97, H 6.00, N 9.33; found: C 76.97, H 6.17, N 9.19.

Synthesis of *p*-bromophenyldimestylborane (7a): Yield 81%; ^{1}H NMR ($CDCl_3$, 25 °C): δ = 7.51 (d, J = 4.2 Hz, 2H), 7.40 (d, J = 4.2 Hz, 2H), 6.84 (s, 4H), 2.33 (s, 6H), 2.01 (s, 12H) ppm.

Synthesis of *p*-[3,5-bis(2,2′-dipyridylamino)phenyl]phenyldimesitylborane (7): A hexane solution of *n*BuLi (1.6 M, 0.73 mL, 1.2 mmol) was added at −78 °C to a THF (20 mL) solution of **7a** (0.410 g, 1.0 mmol). After being stirred for 1 h at this temperature, the cold mixture was cannulated into a solution of $B(OMe)_3$ (0.3 mL, 3.6 mmol) in THF (20 mL) at −78 °C. After the mixture had been stirred for another 1 h at −78 °C, it was al-

lowed to warm to ambient temperature and stirred overnight. The solution was partitioned between saturated aqueous NH_4Cl (30 mL) and CH_2Cl_2 (30 mL). The aqueous layer was extracted further with CH_2Cl_2 (2×30 mL) and the combined organic layers were dried over $MgSO_4$. The product was purified by flash chromatography (THF/hexane, 1:2) to provide the boronic acid in 60% yield. A mixture of 3,5-bis(2,2′-dipyridylamino)bromobenzene (0.125 g, 0.25 mmol), $[Pd(PPh_3)_4]$ (0.025 g, 0.022 mmol), and toluene (40 mL) was stirred for 10 min. The above boronic acid (185 mg, 0.5 mmol) in 20 mL of EtOH and NaOH (0.8 g) in 20 mL of H_2O were subsequently added. The mixture was stirred and heated at reflux for 40 h and allowed to cool to room temperature. The water layer was separated and extracted with CH_2Cl_2 (3×30 mL). The combined organic layers were dried over $MgSO_4$, and the solvents were evaporated under reduced pressure. Purification of the crude product by column chromatography (THF/hexane 2:1) afforded **7** as a colorless solid in 21% yield; m.p. 141–143°C; ^{1}H NMR ($CDCl_3$, 25°C): δ = 8.35 (d, J = 3.3 Hz, 4H), 7.59 (t, J = 7.2 Hz, 4H), 7.51(d, J = 8.1 Hz, 2H), 7.44(d, J = 8.1 Hz, 2H), 7.29 (d, J = 1.8 Hz, 2H), 7.13 (d, J = 8.1 Hz, 4H), 7.00 (t, J = 1.8 Hz, 1H), 6.96 (t, J = 6.0 Hz, 4H), 6.82 (s, 4H), 2.32 (s, 6H), 2.00 (s, 12H) ppm; ^{13}C NMR ($CDCl_3$, 25°C): δ = 158.2 148.9, 146.7, 145.3, 143.8, 143.6, 142.1, 141.2, 139.0, 138.1, 137.2, 128.6, 127.0, 124.8, 122.5, 118.9, 117.85, 23.8, 23.6 ppm; elemental analysis calcd (%) for $C_{50}H_{45}BN_6\cdot 0.3\,CH_2Cl_2$: C 78.85, H 5.98, N 10.97; found: C 79.07, H 5.83, N 10.87.

Synthesis of *p*-(2,2′-dipyridylamino)-2-thienylbenzene (8a): Diisobutylaluminum hydride (1.0 M in hexane, 0.32 mL, 0.32 mmol) was added to a THF (10 mL) solution of $[Pd(PPh_3)_2Cl_2]$ (0.11 g, 0.157 mmol). After the solution had been stirred for 10 min, *p*-(2,2′-dipyridylamino)bromobenzene (1.31 g, 4 mmol) in THF (10 mL) was added. After an additional 10 min stirring, 2-thienylzinc bromide (0.50 M in THF, 9 mL, 4.5 mmol) was slowly added by syringe and the mixture was heated at reflux for 6 h. The mixture was allowed to cool to room temperature and poured into a saturated aqueous solution of Na_2CO_3. The aqueous phase was extracted with CH_2Cl_2 (3×20 mL), and the organic extracts were concentrated to give a brown residue, which was purified by column with THF/hexanes (2:3) as the eluent to obtain **8a** (yield 63%); ^{1}H NMR ($CDCl_3$, 25°C): δ = 8.39 (dd, J = 5.1, 1.2 Hz, 2H), 7.57–7.64 (m, 4H), 7.29 (dd, J = 3.6, 2.1 Hz, 2H), 7.22 (dt, J = 8.4, 1.8 Hz, 2H), 7.09 (dd, J = 5.1, 3.6 Hz, 1H), 7.05 (d, J = 8.4 Hz, 2H), 6.98 (ddd, J = 7.2, 5.1, 0.9 Hz, 2H) ppm.

Synthesis of *p*-(2,2′-dipyridylamino)phenyl-2-bromo-5-thiophene (8b): 2,5-Dibromothiophene (0.70 g, 2.89 mmol), $[Pd(PPh_3)_4]$ (0.016 g, 0.014 mmol), and toluene (40 mL) were stirred for 10 min, and *p*-(2,2′-dipyridylamino)phenylboronic acid (0.88 g, 2.75 mmol) in EtOH (15 mL) and Na_2CO_3 (0.60 g) in water (20 mL) were then added. The mixture was heated at reflux for 24 h. After it had been allowed to cool to room temperature, the aqueous phase was extracted with CH_2Cl_2 (25 mL×3). The extracts were concentrated to give a yellow residue, which was purified by column chromatograph with THF/hexanes (1:1) as the eluent to obtain **8b** (0.90 g, 80% yield); ^{1}H NMR ($CDCl_3$, 25°C): δ = 8.36 (dd, J = 4.8, 1.2 Hz, 2H), 7.50–7.64 (m, 4H), 7.29 (d, J = 9.9 Hz, 1H), 7.21 (ddd, J = 8.7, 4.5, 2.1 Hz, 2H), 7.02–7.10 (m, 3H), 6.96 (ddd, J = 7.2, 4.8, 0.9 Hz, 2H) ppm.

Synthesis of 5-[*p*-(2,2′-dipyridylamino)phenyl]-2-thienyldimesitylborane (8): Use of a procedure similar to that described for **1** provided yellow-green solid **8** in 62% yield from **8b** and 25% from **8a**; m.p. 193–194°C; ^{1}H NMR ($CDCl_3$, 25°C): δ = 8.38 (d, J = 3.6 Hz, 2H), 7.68 (d, J = 8.4 Hz, 2H), 7.60 (ddd, J = 8.1, 7.2, 1.8 Hz, 2H), 7.43–7.46 (m Hz, 2H), 7.20 (d, J = 8.4 Hz, 2H), 7.05 (d, J = 8.1 Hz, 2H), 6.98 (dd, J = 7.2, 2.1 Hz, 2H), 6.89 (s, 4H), 2.39 (s, 6H), 2.18 (s, 12H) ppm; ^{13}C NMR ($CDCl_3$, 25°C): δ = 158.5, 157.3, 150.0, 149.3, 145.8, 142.4, 141.9, 141.5, 139.2, 138.4, 131.8, 128.9, 128.1, 127.7, 125.9, 119.2, 117.9, 24.1, 21.9 ppm; elemental analysis calcd (%) for $C_{38}H_{36}BSN_3\cdot 0.5\,CH_2Cl_2$: C 74.57, H 5.97, N 6.78; found: C 74.70, H 6.48, N 6.24.

Synthesis of (*p*-(2,2′-dipyridylamino)biphenyldimesitylborane){Zn(CF$_3$COO)$_2$} (10): A mixture of compound **2** (20 mg, 0.035 mmol) and $Zn(CF_3COO)_2\cdot 3H_2O$ (0.0108 g, 0.037 mmol) was dissolved in a minimum amount of THF, and a few drops of benzene were then layered. After the solution had been allowed to stand for a few days, colorless crystals were obtained in 59% yield; m.p. 158–160°C; ^{1}H NMR in CD_2Cl_2 (δ, ppm, 25°C): 8.67 (d, J = 4.2 Hz, 2H), 8.00 (d, J = 8.4 Hz, 2H), 7.83 (ddd, J = 9.0, 7.2, 1.8 Hz, 2H), 7.73 (d, J = 8.1 Hz, 2H), 7.64 (m, 4H), 7.31 (t, J = 6.0 Hz, 2H), 6.96 (d, 9.0 Hz, 2H), 6.89 (s, 4H) ppm; ^{13}C NMR ($CDCl_3$, 25°C): δ = 155.4, 146.8, 142.2, 141.5, 140.8, 140.3, 139.6, 139, 138.4, 136.6, 130.1, 129.8, 128.6, 127.8, 126.2, 118.8, 116.6 pm; ^{19}F NMR (25°C): δ = −75.71 ppm; elemental analysis calcd (%) for $C_{44}H_{38}BF_6N_3O_4Zn\cdot C_6H_6$: C 63.83, H 4.68, N 4.47; found: C 63.82, H 4.79, N 4.45.

Synthesis of {*p*-(7-azaindolyl)biphenyldimesitylborane}$_2$(AgNO$_3$) (11): A minimal amount of dichloromethane was used to dissolve compound **4** (50 mg, 0.0964 mmol). One molar equivalent (18 mg) of $AgNO_3$ was dissolved in a minimal amount of methanol. The two solutions were mixed and layered with benzene. Light yellow crystals of **11** formed after the solution had been kept at ambient temperature for one week (37% yield); ^{1}H NMR ($CDCl_3$, 25°C): δ = 8.23 (dd, J = 4.95, 1.27 Hz, 1H), 7.85 (dd, J = 7.75, 1.25 Hz, 1H), 7.59 (m, 4H), 7.50 (d, J = 8.50 Hz, 2H), 7.40 (m, 3H), 6.94 (dd, J = 7.85, 5.25 Hz, 1H), 6.896 (s, 4H), 6.66 (d, J = 3.5 Hz, 1H), 2.37 (s, 6H), 2.10 (s, 12H) ppm; ^{13}C NMR (δ, 25°C): 145.9, 145.7, 145.4, 142.3, 142.1, 141.2, 140.4, 139.2, 137.3, 135.5, 131.4, 129.5, 128.7, 126.7, 125.1, 123.0, 117.4, 23.9, 21.7 ppm; elemental analysis calcd (%) for $C_{74}H_{70}B_2N_5O_3Ag\cdot 0.5\,C_6H_6$: C 74.22, H 5.62, N 5.62; found: C 74.03, H 5.91, N 5.32.

Photoluminescent quantum yield measurements: Emission quantum yields were determined relative to 9,10-diphenylanthracene in CH_2Cl_2 at 298 K (Φ_r = 0.95).[21] The absorbances of all samples and the standard at the excitation wavelength were approximately 0.096–0.104. The quantum yields were calculated by previously reported procedures.[22]

X-ray crystallographic analysis: Single crystals of **1**, **3**, and **5–7** were obtained from solutions of CH_2Cl_2 and hexane. Attempts to grow single crystals of **2** and **4** by the same procedure were unsuccessful. Crystals of **10** and **11** were obtained from slow diffusion of benzene/hexane into THF solutions. All crystals were mounted on glass fibers for data collection. Data were collected on a Siemens P4 single-crystal X-ray diffractometer with a CCD-1000 detector and graphite-monochromated $Mo_{K\alpha}$ radiation, operating at 50 kV and 30 mA. Except for the data for compound **11**, collected at 180 K, all data collection was carried out at ambient temperature. The 2θ data collection ranges are ≈3.00–57.00° for all compounds. No significant decay was observed in any samples. Data were processed on a PC with the aid of the Bruker SHELXTL software package[23] (version 5.10) and are corrected for absorption effects. Compounds **1** and **3** belong to the noncentric orthorhombic space group $Pna2_1$ and the noncentric monoclinic space group $P2_1$, respectively. The absolute structure of **1** cannot be reliably determined, while the crystal of compound **3** was determined to consist of one enantiomer only, based on the refinement of the Flack parameter. The remaining compounds all belong to the centric triclinic space group $P\bar{1}$. All structures were solved by direct methods. Disordered CH_2Cl_2 solvent molecules are located in the crystal lattices of **6** and **7**. For compound **7**, the crystal decays rapidly during data collection and the disordered solvent molecules could not be completely modeled and refined, which contributed to the poor quality of the structural data. One benzene solvent molecule per molecule of **10** was located in the crystal lattice and was refined successfully. Disordered hexane and partially disordered solvent molecules were found in the crystal lattice of **11** (3 benzene, 0.5 hexane per molecule of **11**). The disordering of some of the solvent molecules in **11** could not be fully modeled. The CF_3 groups in **10** display rotational disordering, which was modeled and refined successfully. All non-hydrogen atoms except those on some of the disordered solvent molecules were refined anisotropically. The positions of hydrogen atoms were either located directly from difference Fourier maps or calculated and their contributions in structural factor calculations included.

CCDC-222528 (**1**), CCDC-222529 (**3**), CCDC-222530 (**5**), CCDC-222531 (**6**), CCDC-222532 (**7**), CCDC-222533 (**10**), and CCDC-222534 (**11**) contain the supplementary crystallographic data for this paper. These data can be obtained free of charge via www.ccdc.cam.ac.uk/conts/retrieving.html (or from the Cambridge Crystallographic Data Centre, 12 Union Road, Cambridge CB2 1EZ, UK; fax: (+44) 1223-336033; or deposit@ccdc.cam.uk).

Fabrication of electroluminescent devices: The EL devices with **2** or **8** as the emitting layer and the electron-transport layer were fabricated on an indium/tin oxide (ITO) substrate. Organic layers were deposited on the substrate by conventional vapor vacuum deposition. Prior to the deposi-

tion, all organic materials were purified by a train sublimation method.[24] *N,N′*-Bis(1-naphthyl)-*N,N′*-diphenylbenzidine (NPB) was employed as the hole-transport layer in all devices. 2-(4-Biphenyl)-5-(4-*tert*-butylphenyl)-1,3,4-oxadiazole (PBD) was used as the electron-transport layer in one of the devices (device 3). *N,N′*- 4,4′-Bicarbazole-biphenyl (Bicarb) was used as the hole blocking layer in devices 2–4. The cathode composed of LiF and Al was deposited on the substrate by conventional thermal vacuum deposition. The active device area is $1.0 \times 5.0\ mm^2$. The current/voltage characteristics were measured with a Keithley 238 Source Measure Unit. The EL spectra and the luminance for the devices were measured with a Photo Research-650 Spectra Colorimeter.

Acknowledgement

We thank the Natural Sciences and Engineering Research Council of Canada for financial support.

[1] C. D. Entwistle, T. B. Marder, *Angew. Chem.* **2002**, *114*, 3051; *Angew. Chem. Int. Ed.* **2002**, *41*, 2927–2931.
[2] a) Z. Yuan, N. J. Taylor, R. Ramachandran, T. B. Marder, *Appl. Organomet. Chem.* **1996**, *10*, 305–316; b) Z. Yuan, J. C. Collings, N. J. Taylor, T. B. Marder, *J. Solid State Chem.* **2000**, *154*, 5–12; c) Z. Yuan, N. J. Taylor, T. B. Marder, I. D. Williams, S. K. Kurtz, L. T. Cheng, in *Organic Materials for Non-linear Optics, II* (Eds.: R. A. Hann, D. Bloorp), pp 190—194, RSC, Cambridge, **1991**.; d) Z. Yuan, N. J. Taylor, T. B. Marder, I. D. Williams, S. K. Kurtz, L. T. Cheng, *J. Chem. Soc. Chem. Commun.* **1990**, 1489–1492.
[3] a) C. Branger, M. Lequan, R. M. Lequan, M. Large, F. Kajzar, *Chem. Phys. Lett.* **1997**, *272*, 265–270; b) C. Branger, M. Lequan, R. M. Lequan, M. Barzoukas, A. Fort, *J. Mater. Chem.* **1996**, *6*, 555–558.; c) M. Lequan, R. M. Lequan, K. C. Ching, A. C. Callier, M. Barzoukas, A. Fort, *Adv. Mater. Opt. Electron.* **1992**, *1*, 243–247; d) M. Lequan, R. M. Lequan, K. C. Ching, M. Barzoukas, A. Fort, H. Lahoucine, G. Bravic, D. Chasseau, J. Gaultier, *J. Mater. Chem.* **1992**, *2*, 719–725; e) M. Lequan, R. M. Lequan, K. C. Ching, *J. Int. Biomed. Inf. Data* **1991**, *1*, 997–999; f) Z. Q. Liu, Q. Fang, D. Wang, G. Xue, W. T. Yu, Z. S. Shao, M. H. Jiang, *Chem. Commun.* **2002**, 2900–2901.
[4] a) T. Noda, Y. Shirota, *J. Am. Chem. Soc.* **1998**, *120*, 9714–9175; b) T. Noda, H. Ogawa, Y. Shirota, *Adv. Mater.* **1999**, *11*, 283–285; c) Y. Shirota, M. Kinoshita, T. Noda, K. Okumoto, T. Ohara, *J. Am. Chem. Soc.* **2000**, *122*, 11021–11022; d) T. Noda, Y. Shirota, *J. Lumin.* **2000**, *87*, 1168–1170; e) M. Kinoshita, H. Kita, Y. Shirota, *Adv. Funct. Mater.* **2002**, *12*, 780–786; f) H. Doi, M. Kinoshita, K. Okumoto, Y. Shirota, *Chem. Mater.* **2003**, *15*, 1080–1089; g) Y. Shirota, *J. Mater. Chem.* **2000**, *10*, 1–25.
[5] a) S. Yamaguchi, S. Akiyama, K. Tamao, *J. Am. Chem. Soc.* **2001**, *123*, 11372–11375; b) *J. Am. Chem. Soc.* **2000**, *122*, 6335–6336; c) S. Yamaguchi, T. Shirasak, S. Akiyama, K. Tamao, *J. Am. Chem. Soc.* **2002**, *124*, 8816–8817; d) Y. Kubo, M. Yamamoto, M. Ikeda, M. Takeuchi, S. Shinkai, S. Yamaguchi, K. Tamao, *Angew. Chem.* **2003**, *115*, 2082; *Angew. Chem. Int. Ed.* **2003**, *42*, 2036–2040.
[6] a) A. B. Chwang, R. C. Kwong, J. J. Brown, *Phys. Lett.* **2002**, *80*, 725–727; b) N. K. Patel, S. Cina, J. H. Burroughes, *IEEE, J. Selected Topics in Quantum Electronics* **2002**, *8*, 346–361; c) T. Tsutsui, K. Fujita, *Adv. Mater.* **2002**, *14*, 949–952; d) O. Nuyken, E. Bacher, T. Braig, R. Faber, F. Mielke, M. Rojahn, V. Wiederhirn, K. Meerholz, D. Muller, *Design. Monomers and Polymers*, **2002**, *5*, 195–210; e) S. Miyata, Y. Sakuratani, X. T. Tao, *Opt. Mater.* **2003**, *21*, 99–107.
[7] C. W. Tang, S. A. Van Slyke, *Appl. Phys. Lett.* **1987**, *51*, 913–915.
[8] W. L. Jia, D. T. Song, S. Wang, *J. Org. Chem.* **2003**, *68*, 701–705.
[9] a) J. Pang, Y. Tao, S. Freiberg, X. P. Yang, M. D'Iorio, S. Wang, *J. Mater. Chem.* **2002**, *12*, 206–212.; b) C. Seward, J. Pang, S. Wang, *Eur. J. Inorg. Chem.* **2002**, 1390–1399; c) J. Pang, E. J. P. Marcotte, C. Seward, R. S. Brown, S. Wang, *Angew. Chem.* **2001**, *113*, 4166; *Angew. Chem. Int. Ed.* **2001**, *40*, 4042–4045; d) S. Wang, *Coord. Chem. Rev.* **2001**, *215*, 79–98; e) W. Yang, H. Schmider, Q. Wu, Y. Zhang, S. Wang, *Inorg. Chem.* **2000**, *39*, 2397–2404; f) Q. Wu, M. Esteghamatian, N. X. Hu, Z. Popovic, G. Enright, S. R. Breeze, S. Wang, *Angew. Chem.* **1999**, *111*, 1038–1041; *Angew. Chem. Int. Ed.* **1999**, *38*, 985–988.
[10] a) N. Miyaura *Adv. Met.-Org. Chem.* **1998**, *6*, 187–243, and references therein. b) A. Suzuki, *J. Organomet. Chem.* **1999**, *576*, 147–168, and references therein.
[11] a) Y. Kang, S. Wang, *Tetrahedron Lett.* **2002**, *43*, 3711–3713; b) Y. Kang, D. Song, H. Schmider, S. Wang, *Organometallics* **2002**, *21*, 2413–2421; c) H. B. Goodbrand, N. X. Hu, *J. Org. Chem.* **1999**, *64*, 670–674; d) J. Lindley, *Tetrahedron* **1984**, *40*, 1433; e) P. E. Fanta, *Synthesis* **1974**, *1*, 9–21.
[12] a) M. M. Olmstead, P. P. Power, *J. Am. Chem. Soc.* **1986**, *108*, 4235–4236; b) R. A. Bartlett, P. P. Power, *Organometallics* **1986**, *5*, 1916–1917; c) A. Pelter, R. Drake, M. Stewart, *Tetrahedron* **1994**, *50*, 13829–13846; d) A. Pelter, L. Warren, J. W. Wilson, *Tetrahedron* **1993**, *49*, 2988–3006; e) K. Okada, T. Sugawa, M. Oda, *J. Chem. Soc. Chem. Commun.* **1992**, 74–75; f) S. Yamaguchi, T. Shirasaka, K. Tamao, *Org. Lett.* **2000**, *2*, 4129–4132.
[13] J. Pommerehne, H. Vestweber, W. Guss, R. F. Mahrt, H. Bassler, M. Porsch, J. Daub, *Adv. Mater.* **1995**, *7*, 551–554.
[14] Gaussian 98 (Revision A.7), M. J. Frisch, G. W. Trucks, H. B. Schlegel, G. E. Scuseria, M. A. Robb, J. R. Cheeseman, V. G. Zakrzewski, J. A. Montgomery, Jr., R. E. Stratmann, J. C. Burant, S. Dapprich, J. M. Millam, A. D. Daniels, K. N. Kudin, M. C. Strain, O. Farkas, J. Tomasi, V. Barone, M. Cossi, R. Cammi, B. Mennucci, C. Pomelli, C. Adamo, S. Clifford, J. Ochterski, G. A. Petersson, P. Y. Ayala, Q. Cui, K. Morokuma, D. K. Malick, A. D. Rabuck, K. Raghavachari, J. B. Foresman, J. Cioslowski, J. V. Ortiz, B. B. Stefanov, G. Liu, A. Liashenko, P. Piskorz, I. Komaromi, R. Gomperts, R. L. Martin, D. J. Fox, T. Keith, M. A. Al-Laham, C. Y. Peng, A. Nanayakkara, C. Gonzalez, M. Challacombe, P. M. W. Gill, B. G. Johnson, W. Chen, M. W. Wong, J. L. Andres, M. Head-Gordon, E. S. Replogle, J. A. Pople, Gaussian, Inc., Pittsburgh, PA, **1998**.
[15] D. E. Wong, T. H. Dunning, Jr., *J. Chem. Phys.* **1993**, *98*, 1358–1371.
[16] MOLEKEL 4.1, P. Flkiger, H. P. Lthi, S. Portmann, J. Weber, Swiss Center for Scientific Computing, Manno (Switzerland), **2000**–**2001**.
[17] S. F. Liu, Q. Wu, H. L. Schmider, H. Aziz, N. X. Hu, Z. Popovic, S. Wang, *J. Am. Chem. Soc.* **2000**, *122*, 3671–3678.
[18] C. Seward, J. Chan, D. Song, S. Wang, *Inorg. Chem.* **2003**, *42*, 1112–1120.
[19] R. J. Lancashire, in *Comprehensive Coordination Chemistry* (Eds.: G. Wilkison, R. D. Gillard, J. A. McCleverty), Pergamon, Oxford, **1987**, Vol. 5, ch. 54.
[20] Q. Wu, J. A. Lavigne, Y. Tao, M. D'Iorio, S. Wang, *Chem. Mater.* **2001**, *13*, 71–77.
[21] S. L. Murov, I. Carmichael, G. L. Hug, *Handbook of Photochemistry*, 2nd ed., Marcel Dekker, New York, **1993**.
[22] N. J. Demas, G. A. Crosby, *J. Am. Chem. Soc.* **1970**, *92*, 7262–7270.
[23] SHELXTL NT Crystal Structure Analysis Package, Version 5.10; Bruker Axs, Analytical X-ray System, Madison, WI, **1999**.
[24] H. J. Wagner, R. O. Loutfy, C. K. Hsiao, *J. Mater. Sci.* **1982**, *17*, 2781–2791.

Received: September 27, 2003 [F5579]